INTERNATIONAL JOURNAL OF HYDROGEN ENERGY 46 (2021) 8995–9007

Available online at www.sciencedirect.com

ScienceDirect

journal homepage: www.elsevier.com/locate/he

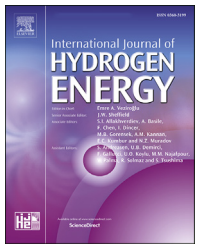

Exergy analysis of glycerol steam reforming in a heat recovery reactor

Felipe Pinheiro Falcão Dias [a], *Igor Teles Fernandes* [a], *André Valente Bueno* [a,*], *Paulo Alexandre Costa Rocha* [a], *Mona Lisa Moura de Oliveira* [b]

[a] *Universidade Federal Do Ceará, Departamento de Engenharia Mecânica, Campus Do Pici 715, Fortaleza, CE, 60440-554, Brazil*

[b] *Universidade Estadual Do Ceará, Centro de Ciências e Tecnologia, Campus Itaperi, Fortaleza, CE, 60.714-903, Brazil*

HIGHLIGHTS

- Detailed exergy analysis of glycerol steam reforming.
- Syngas maximum exergy value and efficiency coincided with maximum hydrogen yield.
- Experiments indicate a maximum reforming exergy efficiency of 75.8%.
- Trade-off between irreversibilities and tar exergy losses was evidenced.

ARTICLE INFO

Article history:
Received 31 August 2020
Received in revised form
14 December 2020
Accepted 30 December 2020
Available online 22 January 2021

Keywords:
Exergy analysis
Heat recovery steam reforming
Hydrogen production
Glycerol reforming
Biodiesel sub-product

ABSTRACT

A detailed exergy analysis was performed for the steam reforming process of glycerol by means of a series of experiments in a bench scale apparatus. The reforming was conducted in a fixed bed reactor, which operated in heat recovery mode by extracting the demanded energy from hot exhaust gases provided by a diesel engine. In order to determine the role of the main operational parameters into the exergy efficiency of the studied process, the experiments were carried out with glycerol feed concentrations in water ranging from 10% up to 90% weight, whereas the outlet reactor temperature was varied from 600 °C up to 800 °C. Detailed exergy balances revealed a compromise between the exergy destruction within the reforming reactor and liquid separator versus the exergy losses associated to the tar and char outputs. This trade-off was favourable to the 50% and 70% glycerol feed concentration regimes and plateaus of about 74% exergy efficiency and 24 MJ/kg dry syngas exergy content were verified from 650 to 800 °C reactor temperatures.

* *Corresponding author.*
E-mail address: bueno@ufc.br (A.V. Bueno).

https://doi.org/10.1016/j.ijhydene.2020.12.215

Introduction

The current fast-growing demand for renewable energy sources is believed to be maintained as a response to the environmental concerns raised by the widespread fossil fuels utilisation [1]. Biofuels are an important part of this initiative and play a key role in mobility applications, as the fossil fuel production tends to lose dominance due to its environmental footprint and supply insecurity [2]. Biodiesel and ethanol are currently leading this initiative in the mobility sector. These fuels require slight or no modifications in the physical structure of the engines and its production technologies are relatively straightforward. Furthermore, the existing fuel delivery infrastructure has been successfully applied to supply these biofuels to the points of consumption [3].

A wide diversity of feedstock alternatives is currently available to meet the biofuels demand when one takes biodiesel into account: vegetable oils [4,5], waste oil [6], animal fat [7] and algae [8]. Despite the diversity of characteristics of the raw materials accessible for biodiesel industrial plants, a single reaction route, which is denominated transesterification, practically dominates its large scale production [9]. In the transesterification process a triglyceride reacts with a short-chain alcohol in the presence of a catalyst to form biodiesel and the sub-product glycerol. There is a general consensus that finding an adequate destination to the huge amounts of glycerol resulting from biodiesel production poses a critical issue to the development of environmental friendly and efficient biorefinery plants [10,11]. Glycerol destination is closely related to the sustainability of biodiesel industry, a factor that, together with deforestation and food competition issues, is currently moulding the future of the biodiesel production chain [12].

In order to achieve the standards required for its application in chemical industries, the glycerol generated in biodiesel production plants, denominated crude glycerol, demands an expensive purification process designed to remove methanol, catalyst and salt traces [13]. For that reason, glycerin synthesized by other routes has a relatively lower cost in comparison to the raw material obtained by recycling the crude glycerol [14]. This scenario prevented the traditional uses of glycerol from being capable of absorbing the overproduction coming from biodiesel industry and posed its discharge management as a challenge to biodiesel sustainability [15]. Therefore, it is crucial to develop alternative applications for the crude glycerol in order to limit oversupply [16], which otherwise could threaten the environmental benefits of replacing fossil fuels by biodiesel [17].

Thermal processes such as pyrolysis and steam reforming have received increasing attention as means for glycerol management in biorefineries [9,18–20]. Glycerol has high hydrogen content [21] and can be processed to syngas at relatively low temperatures due to the presence of oxygen on its formulation [22]. Promising results in terms of efficiency gains and lower emissions have been reported with the integration of glycerol reforming systems, power generating units and biodiesel production plants [23]. According to Reza Ziyai et al. [24], to perform the crude glycerol reforming and then convert the produced hydrogen into electricity can increase the economic viability of biodiesel plants. Cormos et al. [25] evaluated the techno-economic and environmental performances of hydrogen and power generation based on glycerol steam reforming with and without carbon capture. These authors demonstrated that hydrogen and power co-generation are a promising option to further increase the overall energy efficiency and to improve the plant flexibility. Matson and co-workers [26] have shown that a biodiesel plant can also become self-sufficient, from the electric power point of view, by using syngas obtained from glycerol to operate a dual fuel electric generator.

Beyond the opportunities of improving the biodiesel production chain, hydrogen production via glycerol could also take part of a smooth transition process leading to a renewable hydrogen economy, in contrast to the current scenario where fossil fuels predominate as raw material. In fact, the relevance of hydrogen energy field appears to mould the research efforts dedicated to the syngas production from glycerol and, in consequence, most of the attention dedicated to the study of its thermal processing has been focused in obtaining a high hydrogen yield. As stated in the review by Silva et al. [27], aspects such as the optimisation of process parameters [28–30], novel reactor designs [31–33] and the use of advanced catalysts [34–36] have received considerable interest.

To guarantee that the glycerol reforming process achieves acceptable levels of energy efficiency is another relevant operational aspect, perhaps as important as obtaining a high hydrogen yield. Interestingly, the number of studies dedicated to this subject is still limited and the currently available works share the same methodology: numerical simulations adopting the Gibbs free energy minimization method [37–39]. In a recent work, Pashchenko and collaborators [37] calculated the energy efficiency of biofuels steam reforming using waste-heat recuperation as energy source. Their results indicate a maximum energy efficiency of 62.5% to the glycerol reforming, which was obtained at 627 °C with a water to glycerol ratio of 1:5 wt and a pressure of 1 bar. Hajjaji et al. carried a detailed thermodynamic analysis of the hydrogen production via thermochemical processing of glycerol by simulating both its steam and autothermal reforming within isothermal reactors [38,39]. They registered a maximum exergy efficiency level of 67.8% for the autothermal reforming, which was achieved at 627 °C, 1.08 water to glycerol feed ratio and 0.33 oxygen to glycerol ratio [38]. In the steam reforming process, the authors recommend a temperature of 827 °C and a water to glycerol feed ratio of 1.17 that corresponds to a maximum exergy efficiency of 66.1% [39].

Previous works demonstrate that glycerol decomposition is an endothermic process that requires high temperature and a considerable concentration of water to achieve adequate levels of hydrogen production, conditions that are not favourable to the operation of the reforming system at high values of energy efficiency. Thus, simultaneously complying with hydrogen yield and thermodynamic efficiency requirements can be a very challenging task that would demand an advanced diagnosis approach. Valuable information regarding the effects of operational parameters upon the reforming system efficiency can be obtained via exergy analysis, a well stablished thermodynamic method that is widely

used for process evaluation and rationalisation [40]. Indeed, the exergy analysis method has been successfully applied in a number of recent studies dedicated to the reforming of coal [41], biomass [42] and ethanol [43,44].

Motivation, novelty and research objectives

In this study, the thermodynamic efficiency of the glycerol steam reforming was evaluated by means of a series of experiments carried out in a bench-scale heat-recovery reactor. Waste heat from the exhaust gases produced by an internal combustion engine was used as the energy source to perform the glycerol reforming. Besides the benefits associated to energy conservation, the use of heat recovery to proceed the glycerol gasification also aimed at better reproducing practical conditions where output hot gases losses and a non-homogeneous bed temperature profile are present. Energy and exergy balances were conducted for the complete system and its main components with the objective of establishing cause and effect relationships between relevant operational parameters and the reforming thermodynamic efficiency. The experimental procedures adopted here are also expected to better capture the effects of tar and solid carbon (char) formation in comparison to the equilibrium simulation methods currently in use, making it possible to reach glycerol to water feed ratios of up to 9:1 with acceptable accuracy.

Materials and methods

A series of steady state experiments was performed in a bench scale fixed bed reforming reactor operating with glycerol. Each component of the reforming system was instrumented to provide the data required to analyse the degree of thermodynamic perfection involved in the production of synthesis gas suitable for use as a fuel. A National Instruments SCXI system was used to perform the signal conditioning and data acquisition tasks and the user interface was built with the LabView software. Real time closed loop control was implemented to the fuel metering and waste heat systems. A schematic representation of the experimental apparatus adopted in this work can be found in Fig. 1.

The reforming process configuration considered here will be described toward the glycerol and syngas paths. A liquid solution of glycerol (99,5% purity) into deionised water was delivered to the reactor by means of a computer controlled injection system composed by an automotive fuel pump, a pressure relief valve and a solenoid operated pintle-type fuel injector. The reactants were injected at a constant pressure (3.5 bar(g)) and with variable flow rate, which was controlled through the pulse width modulation technique applied on the solenoid injector. Each experimental regime received a specific mass flow set point that was previously calculated in order to maintain a constant residence time of 4s in all of the experiments. The residence time calculations took the thermodynamic state of the water vapour at the reactor outlet as reference. The reactants mass flow and density were measured with a Siemens FC300 DN4 Coriolis flow meter that also provided the output signal demanded for closed-loop control of the feed injection rate.

A water-cooled head was employed to proceed with the glycerol-water mixture injection, vaporisation and distribution across the reactor bed inlet surface. The fuel injector was centrally mounted at the top of the head and its spray impinged a bowl-shaped vaporisation pre-chamber operating at ca. 400 °C. The gaseous mixture leaving the pre-chamber was directed to the reaction bed by a series of vapour channels. Glycerol reforming occurred in a cylindrical reactor with 94 mm of internal diameter and 500 mm height. The reactor was packed with nickel/alumina spheres of 1.5 mm diameter with 18 2 wt% Ni content (Gunina Engineers, India). In order to discard any influence of the catalyst deactivation effects, the reforming reactor was filled with brand new packing material that was in situ reduced in H2/N2 flow before each experimental run. A total of 70.5 kg of packing material was consumed through the complete set of experiments. A filtering plate with multiple 0.4 mm orifices supported the reaction bed.

The reforming reaction received waste-heat from combustion products provided by an internal combustion engine. The complete heat-recovery reformer had a construction similar to a shell and tube heat exchanger, with one pass in the inner tube corresponding to the reaction bed and 21 passes of exhaust gases in its shell-side. Heat losses to the surroundings were prevented by using a ceramic foam insulation sleeve mounted outside the exhaust gases labyrinth. In order to endure the high temperatures involved in the studied process, the injection head, the heat-recovery reactor and external tubing were all build in AISI 310 stainless steel. Inconel k-type thermocouple probes were placed at the evaporation chamber, reaction bed inlet, reaction bed outlet, exhaust gases inlet and exhaust gases outlet. Pressure measurements were also conducted at these points with piezoresistive transducers (Omega PXM409) with an accuracy of 0.11 kPa.

Reforming temperature is a fundamental operational parameter and, accordingly, the experiments were performed at prescribed values of reactor outlet temperature that were maintained with a repeatability of 10 K. The DAQ and control system adjusted this temperature by actuating in the amount of hot exhaust gases delivered by an internal combustion engine to the reforming reactor. The engine used for the experiments was a high-speed diesel (see Table 1) and it was operated at full throttle conditions, while the control system actuated in the amount of brake torque that was applied by an alternate current dynamometer. The engine exhaust gas flow was indirectly computed with 27 g/min uncertainty from combined measurements conducted with an Omega FMA-900-V intake air flow meter and a Siemens FC300 fuel flow meter. The exhaust gases temperatures at the heat recovery circuit inlet and outlet were measured with Inconel k-type thermocouple probes with an accuracy of 0.62 K. Further details regarding the reactor construction can be found in a previous work of Bueno and Oliveira [22].

The high temperature wet syngas produced in the experiments was diverted to a water-cooled condenser in order to separate its gaseous fraction from the liquid and solid ones. This device is a cylindrical separator with a fixed bed of 0.9 dm^3 filled with the reactor's packing material and surrounded by a high flow cooling water jacket. The liquid

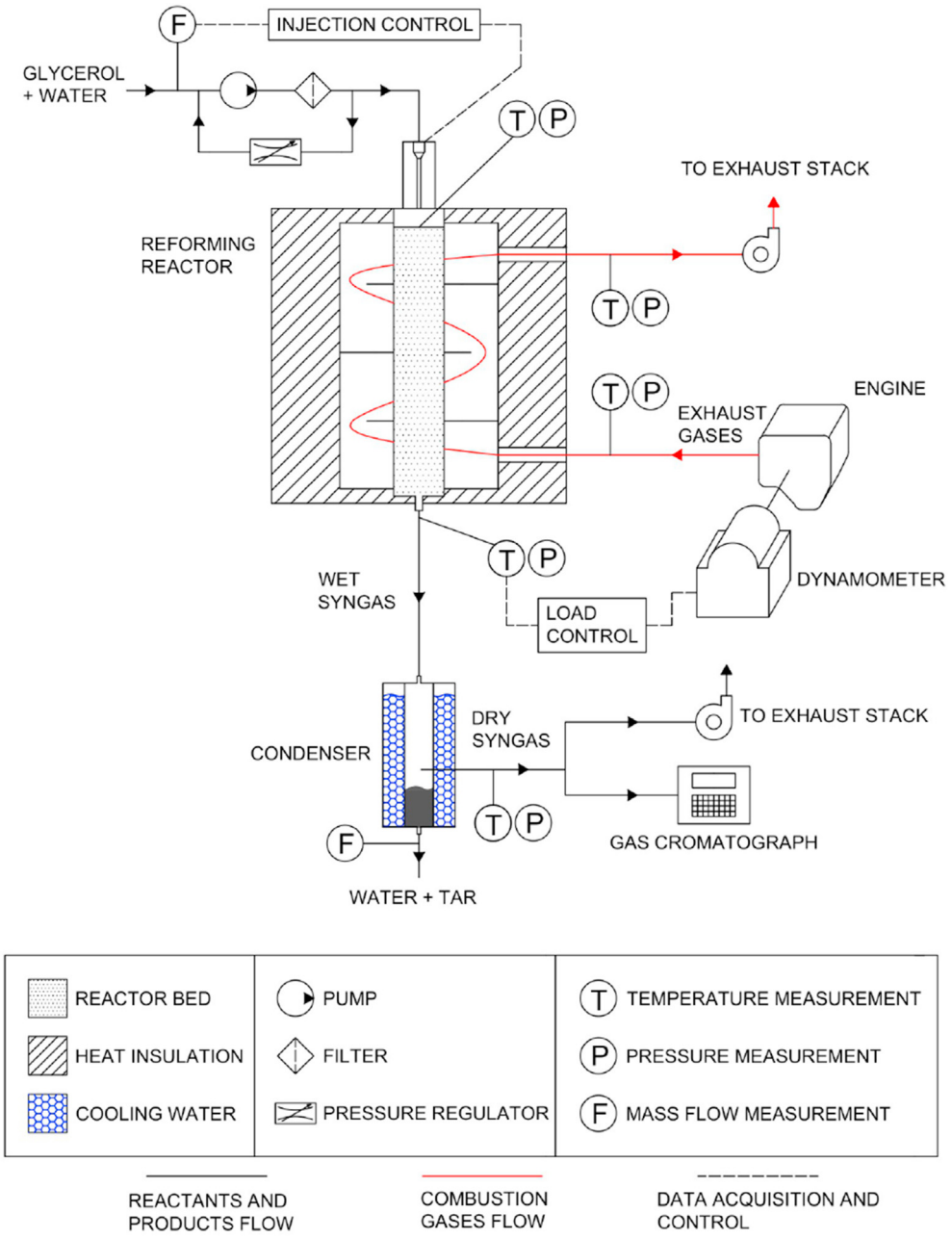

Fig. 1 – Schematic representation of the experimental setup.

Table 1 – Engine specifications.

Configuration	Single Cylinder High-Speed Naturally Aspirated
Cycle	Air Cooled 4 stroke
Injection System	Mechanical - Direct Injection
Bore x Stroke (mm)	78 × 62
Compression Rate	23:1
Adopted Fuel	Soybean Oil Methyl Ester
Maximum Brake Power (kW)	4,25 kW @ 3694 rpm
Thermal Efficiency at Maximum Brake Power	19.37%

fraction mass flow and density were measured with a Siemens FC300 DN4 Coriolis flow meter. The solid carbon accumulated in the reactor and condenser beds was rinsed after the end of each experimental run, separated by the paper filter technique, dried and determined by direct weighting. Total carbon analysis was applied to the liquid fraction using a HACH Spectrophotometer DR 2800 with MR direct method.

The dry syngas left the condenser at room temperature and was directed to an exhaust device, while a small sample was sent to a gas chromatograph (GC Varian CP 3800) in order to determine its composition. A thermal conductivity detector (TCD) was used for hydrogen, carbon dioxide and carbon monoxide analysis, whereas light hydrocarbons were computed by a flame ionisation detector (FID) with oven

temperature of 350 °C and a capillary column of the CP-Sil 5 CB type. The variability observed in the mole fractions obtained by the gas chromatography analysis was always less than 2%.

The uncertainties associated to thermodynamic quantities such as the syngas exergy and the exergy efficiencies were calculated from the contributions of each measured variable demanded for its determination, according to Ref. [45]:

$$w_A = \left[\left(\frac{\partial A}{\partial x_1}w_1\right)^2 + \left(\frac{\partial A}{\partial x_2}w_2\right)^2 + \cdots + \left(\frac{\partial A}{\partial x_n}w_n\right)^2\right]^{1/2} \quad (1)$$

where A represents the calculated thermodynamic quantity, w_A is the uncertainty in the calculated result and w_n stands for a measurement accuracy or an uncertainty in one of the dependent variables. All instruments were properly calibrated before the experiments in order to limit systematic experimental errors, while the accuracies reported within this section for the temperature, pressure and mass flow measurements were directly taken from manufacturer calibration data. Mass balance closures corresponding to the maximum exergy efficiency operational regimes are provided in Table 2 in order to validate the experimental data used in the exergy analysis. The observed closure errors are compatible with the instruments accuracies and in agreement to the ones reported by Yildiz and co-workers using a similar experimental setup [46].

Reaction steps for the glycerol steam reforming

According to Dupont and co-authors [47], the complex reactions involved in the steam reforming of glycerol can be summarised by the simplified mechanism described as follows. The first step is the decomposition of glycerol into syngas:

$$C_3H_8O_3 \overset{H_2O}{\Rightarrow} 3CO + 4H_2 \quad (2)$$

that is followed by the water-gas shifting reaction:

$$CO + H_2O \underset{highT}{\overset{lowT}{\rightleftharpoons}} CO_2 + H_2 \quad (3)$$

Combining (2) with 3x (3) yields the overall steam reforming of glycerol:

$$C_3H_8O_3 + 3H_2O \Rightarrow 3CO_2 + 7H_2 \quad (4)$$

that limits the hydrogen syngas concentration to 70% in conventional steam reforming. Hydrogen can be consumed at low temperature via methanation of CO and CO_2, whereas at high temperatures the reverse reactions of methane steam reforming prevail [39]:

$$CO + 3H_2 \underset{highT}{\overset{lowT}{\rightleftharpoons}} CH_4 + H_2O \quad (5)$$

$$CO_2 + 4H_2 \underset{highT}{\overset{lowT}{\rightleftharpoons}} CH_4 + 2H_2O \quad (6)$$

Exergy analysis

Exergy is the amount of work obtained when a piece of matter is brought to a state of thermodynamic equilibrium with the common components of its surroundings by means of reversible processes. This is a broad definition of exergy, since thermodynamic equilibrium includes not only pressure and temperature but also chemical equilibrium with the substances of the environment [48]. The study of complex and chained processes can be rationalised with the aid of the exergy concept through the so-called exergy analysis, a thermodynamic framework that allows the evaluation of useful effects, resource destruction and losses to the environment on a common basis: the amount of available work.

The molar specific exergy associated to a given flow of matter, known as its flow exergy ($\bar{\epsilon}$), is composed of two distinct contributions: the thermomechanical ($\bar{\epsilon}_{tm}$) and the chemical parcels ($\bar{\epsilon}_{ch}$):

$$\bar{\epsilon} = \bar{\epsilon}_{tm} + \bar{\epsilon}_{ch} \quad (7)$$

The thermomechanical parcel corresponds to the maximum amount of work that can be obtained from a stream when it is brought to thermal and mechanical equilibrium with the reference environment, being given by:

$$\bar{\epsilon}_{tm} = (\bar{h} - \bar{h}_0) - T_0(\bar{s} - \bar{s}_0) \quad (8)$$

where the specific molar properties $\bar{h}_0$ and $\bar{s}_0$ are calculated at the reference environment pressure (P_0) and temperature (T_0) but maintaining the original stream composition unchanged due to the exclusive thermal and mechanical equilibrium restriction. Under such conditions, the stream is said to be at the restricted dead state.

In order to reach the complete equilibrium between the stream and the ambient, further chemical iterations are necessary to match the values of the chemical potentials of each substance in the stream to the ones corresponding to the presence of this same substance in the reference environment. When this condition is attained, the stream is said to have achieved the dead state, which is sometimes referred as unrestricted dead state. The maximum amount of work that can be obtained as the stream goes from its restricted dead state to the complete equilibrium with the reference environment, reaching the dead state, corresponds to its chemical flow exergy. The specific flow chemical exergy can be calculated from:

Table 2 – Mass balance closures.

Feed Ratio	T [°C]	Input Stream [g]	Output Streams [g]				
		Glycerol/Water	Dry Syngas	Water	Tar	Char	Closure Error
50%	700	150.3	60.6	72.5	15.2	0.8	1.2
70%	750	158.9	88.7	47.8	19.3	1.1	2.0

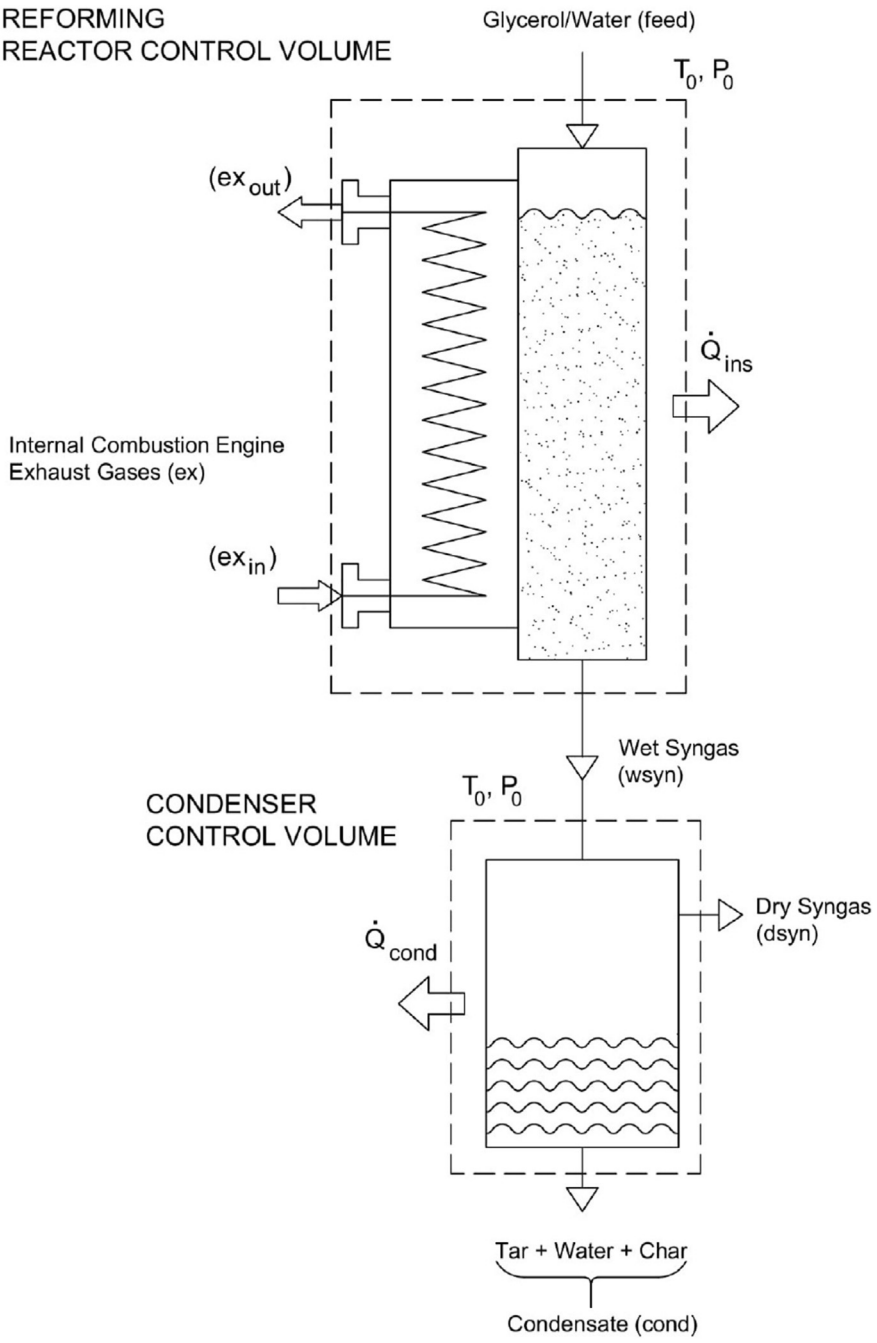

Fig. 2 – Control volumes adopted for the thermodynamic analysis.

$$\bar{\epsilon}_{ch} = \sum_i x_i \bar{\epsilon}_{0,i} + \bar{h}_{mix} + RT_0 \sum_i x_i \ln \gamma_i \cdot x_i \quad (9)$$

In this equation x_i represents the mole fraction of the mixture component i, $\bar{\epsilon}_{0,i}$ its standard chemical exergy and γ_i its activity coefficient. In circumstances where the ideal gas model is a suitable simplification, the enthalpy of mixing ($\bar{h}_{mix}$) becomes null and the activity coefficients are unitary, what causes Eq. (9) to be simplified to:

$$\bar{\epsilon}_{ch} = \sum_i x_i \bar{\epsilon}_{0,i} + RT_0 \sum_i x_i \ln \cdot x_i \quad (10)$$

Two distinct control volumes were adopted for thermodynamic analysis purposes, one corresponding to the heat-recovery reforming reactor and the other to the liquid separator, as can be seen in Fig. 2. Steady state conditions were considered and, for the sake of clarity, the solid carbon formed within the reforming process was assumed to be dispersed into the non-volatile fraction of the products (condensate).

The effects of feed-pumping work were neglected and the control volume surfaces were placed at regions with environment temperature. Furthermore, acetaldehyde was chosen as a surrogate material in the modelling of the tar properties that were demanded in exergy balances containing wet syngas or condensate products. This simplification may be justified by the fact that acetaldehyde has been frequently reported as the main intermediate compound and liquid by-product of the glycerol reforming process [49–51]. Szargut's reference environment model and standard chemical exergies [40] were adopted in the present work.

The irreversibility or exergy destruction rates in the reforming reactor ($\dot{I}_R$) can be obtained from the exergy balance equation applied to the control volume identified in Fig. 2:

$$\dot{N}_{feed}\bar{\epsilon}_{feed} + \dot{N}_{ex_{in}}\bar{\epsilon}_{ex_{in}} - \dot{N}_{ex_{out}}\bar{\epsilon}_{ex_{out}} - \dot{N}_{wsyn}\bar{\epsilon}_{wsyn} - \dot{I}_R = 0 \quad (11)$$

with the molar flow rates ($\dot{N}$) and exergies ($\bar{\epsilon}$) being calculated from experimental data and Eqs. (7) to (10). The water-glycerin (feed) was described as a non-ideal solution with mixing enthalpy and activity coefficients taken from Refs. [52,53], respectively. The ideal gas model was adopted for the engine exhaust hot gases points ex_{in} and ex_{out}, as well as for the syngas flows (*wsyn* and *dsyn*). The thermodynamic properties of the engine exhaust gas were determined by applying a modified version of the PER and EQMD routines proposed by Olikara and Borman [54], as described in Ref. [55]. The wet syngas flow was also considered as an ideal gas mixture composed by hydrogen, carbon monoxide, carbon dioxide, methane, ethylene, acetaldehyde, water and dispersed solid carbon. The specific properties of the syngas constituents were taken from Chemkin II routines [56].

The exergy balance for the liquid separator, or condenser, can be written as follows to determine the exergy destruction:

$$\dot{N}_{wsyn}\bar{\epsilon}_{wsyn} - \dot{N}_{dsyn}\bar{\epsilon}_{dsyn} - \dot{N}_{cond}\bar{\epsilon}_{cond} - \dot{I}_C = 0 \quad (12)$$

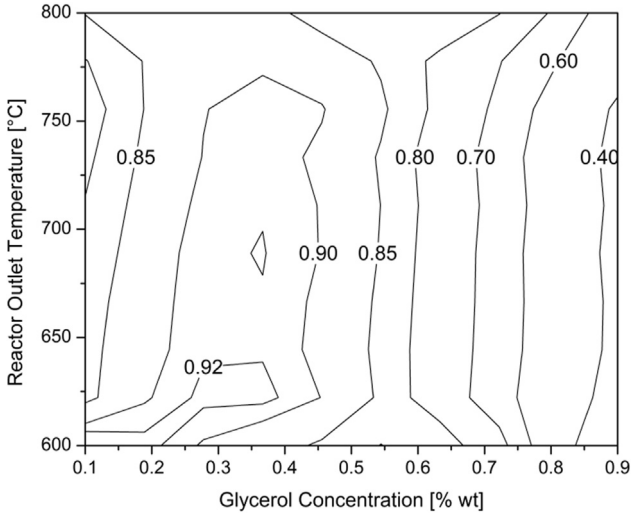

Fig. 3 – Glycerol conversion to gas phase products obtained for the heat-recovery steam reforming of glycerol.

The condensate stream was modelled as a liquid mixture composed by water, the tar surrogate acetaldehyde and dispersed solid carbon. Activity coefficients were taken from Ref. [57] and mixing enthalpies from Ref. [52]. Acetaldehyde concentration was calculated from carbon and hydrogen balances that were performed to the liquid separator with data provided by gas chromatography and total organic carbon analysis of the filtered condensate phase.

Performance metrics

Work and heat transfer terms were not present within the exergy balances, which were restricted to flow and irreversibility terms. Under these conditions, the terms of the exergy balance equations containing exergy inflows are regarded as exergy inputs, while the outflows can be interpreted as useful products or as exergy loses according to its characteristics [40]. Accordingly, the following expression can be written for the reforming reactor efficiency by manipulating Eq. (11):

$$\eta_R = \frac{\dot{N}_{wsyn}\bar{\epsilon}_{wsyn}}{\dot{N}_{feed}\bar{\epsilon}_{feed} + \dot{N}_{ex_{in}}\bar{\epsilon}_{ex_{in}}} = 1 - D_R - L_{ex_{out}} \quad (13)$$

where the normalised values of the exergy destruction within the reactor (D_R) and exhaust gases losses ($L_{ex_{out}}$) are as follows:

$$D_R = \frac{\dot{I}_R}{\dot{N}_{feed}\bar{\epsilon}_{feed} + \dot{N}_{ex_{in}}\bar{\epsilon}_{ex_{in}}} \quad (14)$$

$$L_{ex_{out}} = \frac{\dot{N}_{ex_{out}}\bar{\epsilon}_{ex_{out}}}{\dot{N}_{feed}\bar{\epsilon}_{feed} + \dot{N}_{ex_{in}}\bar{\epsilon}_{ex_{in}}} \quad (15)$$

In a similar way, the liquid separator efficiency is given by:

$$\eta_C = \frac{\dot{N}_{dsyn}\bar{\epsilon}_{dsyn}}{\dot{N}_{wsyn}\bar{\epsilon}_{wsyn}} = 1 - D_C - L_{cond} \quad (16)$$

with the normalised values of exergy destruction (D_C) and combined char and tar losses (L_{cond}) being:

$$D_C = \frac{\dot{I}_C}{\dot{N}_{wsyn}\bar{\epsilon}_{wsyn}} \quad (17)$$

$$L_{cond} = \frac{\dot{N}_{cond}\bar{\epsilon}_{cond}}{\dot{N}_{wsyn}\bar{\epsilon}_{wsyn}} \quad (18)$$

Finally, a global exergy efficiency expression that involves the exergy balance for the complete reforming system can be written by combining Eqs. (11) and (12):

$$\eta_G = \eta_R\eta_C = \frac{\dot{N}_{dsyn}\bar{\epsilon}_{dsyn}}{\dot{N}_{feed}\bar{\epsilon}_{feed} + \dot{N}_{ex_{in}}\bar{\epsilon}_{ex_{in}}} = 1 - D_R - L_{ex_{out}} - D_C - L_{cond} \quad (19)$$

The terms appearing in Eq. (19) were combined to construct Sankey-Grassmann diagrams, which proved to be a useful tool for understanding the effects of operational parameters on the performance of the reforming system.

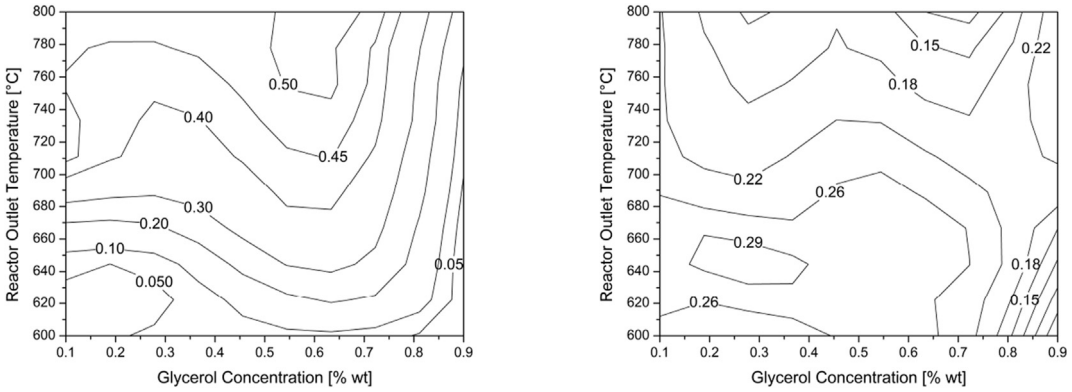

Fig. 4 – Hydrogen and methane concentrations obtained in the dry syngas.

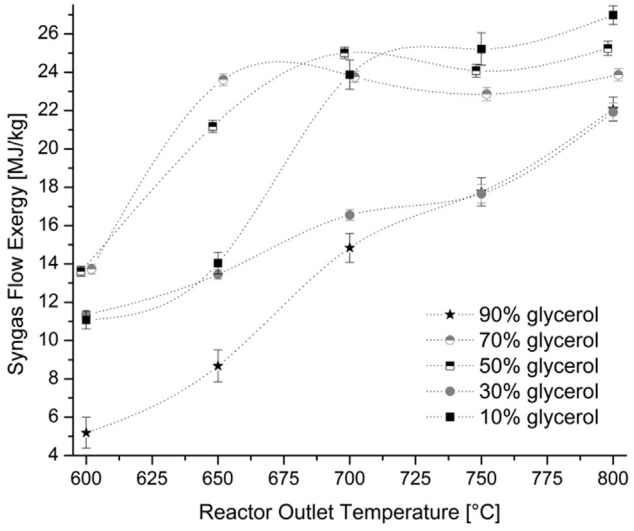

Fig. 5 – Syngas exergy values obtained for the heat-recovery steam reforming of glycerol.

Results and discussion

Synthesis gas composition and exergy content

Glycerol conversion to gas phase products, Fig. 3, reached 84.2 ± 6.4% with the reactor operating at the usual glycerol feed concentrations levels that ranged from 10 up to 70%. Those results corresponded well with data reported by Bobadilla et al. under similar bed material and operational conditions [31]. Further increasing the glycerol ratio to 90% caused water to become a limiting reactant in the wet reforming reactions, while the parallel pyrolysis reactions were still restricted by the relatively low temperature conditions, thus limiting the reforming advance and reducing the gas phase conversion levels to about 30%. In fact, this singular operational condition was inserted in the present work in order to better explore the energy efficiency penalties caused by low levels of gas phase conversion, namely the low value of syngas exergy and the higher than usual tar associated losses.

Contour maps representing the syngas compositions obtained by the experiments are shown in Fig. 4. Hydrogen and

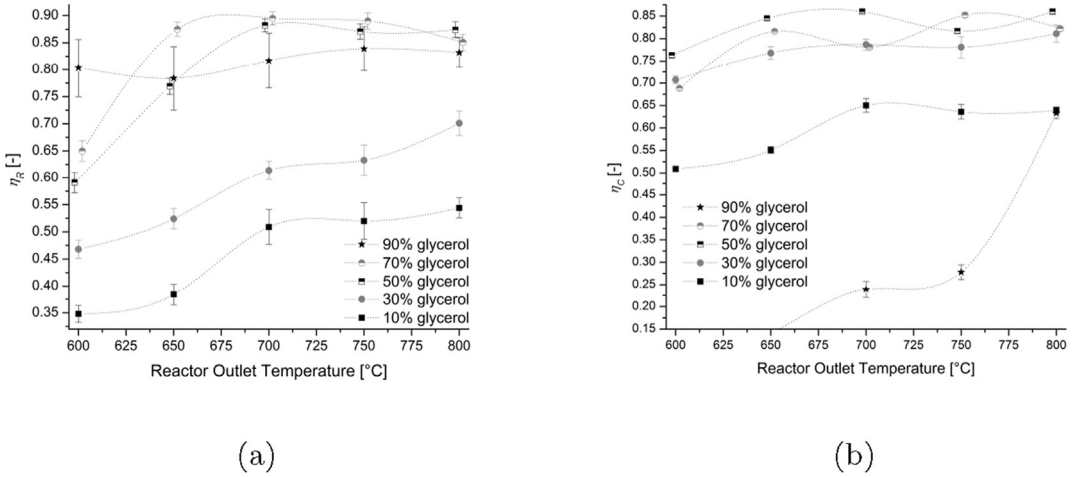

Fig. 6 – Exergy efficiencies obtained for the reforming reactor (η_R) and condenser (η_C).

methane are the most relevant syngas constituents for energy production and, from this figure, it is observed that their yields were oppositely affected by temperature and feed concentration. Methane production was enhanced at relatively low temperatures and glycerol feed concentrations, reaching its maximum at 30% feed concentration and 650 °C. Such conditions lead to methane formation via methanation of CO and CO2 (see Eqs. (5) and (6)), an exothermic mechanism that demands hydrogen consumption. On the other hand, hydrogen production was intensified from 50 to 70% of glycerol feed ratios and reactor temperatures above 750 °C. At such thermodynamic states the exothermic methanation reactions were inhibited in favour of the endothermic glycerol steam reforming overall reaction (Eq. (4)). Further discussion on the role of temperature and feed ratio on the hydrogen and methane production through glycerol reforming can be found in the work of Hajjaji et al. [39].

Synthesis gas with 50–54% hydrogen mole fraction and restricted methane and carbon monoxide contents was obtained at reforming temperatures from 750 to 800 °C and glycerol feed ratios of 50–70%. When compared to the hydrogen mole fractions of 57 ± 3% that are usually reported to micro-scale homogeneously heated reforming reactors operating with alumina supported bed material [29,30,35,50], those results indicate a slight reduction of the hydrogen yield obtained with the heat-recovery reactor configuration. This disparity arises from the non-homogeneous bed temperature profile that is characteristic of the counterflow heating adopted here, which causes the reactor to operate with reduced temperatures at its inlet, a condition that is susceptible to the methane formation in detriment of hydrogen yield.

It can be observed from Fig. 5 that the exergy value of the syngas approaches a maximum threshold of 25 ± 2 MJ/kg for reactor outlet temperature conditions ranging from 700 to 800 °C and glycerol to water feed ratios of 50 and 70%. Taking combustion applications into account, it is interesting to notice that this value represents 135% of the original glycerol exergy value. Pashchenko and co-workers defined a heat transformation coefficient as the ratio between the lower heat values of the syngas and glycerol, reporting a value of 108% at 50% glycerol water feed ratio and 627.13 °C [37]. For the sake of comparison, our experiments indicate a heat transformation coefficient of 98% at this same condition, a value that is 10% lower to the one predicted by the previous authors from equilibrium Gibbs free energy minimization simulations.

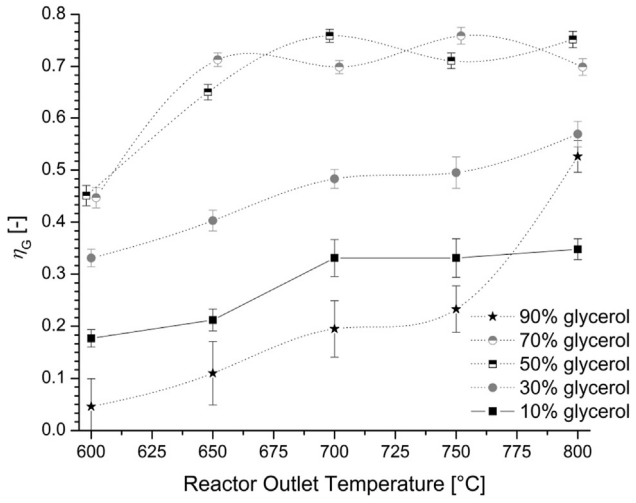

Fig. 7 – Global exergy efficiencies obtained for the heat-recovery steam reforming of glycerol.

Exergy efficiencies

The reforming reactor exergy efficiency generally increased with both glycerol to water feed ratio and reactor outlet temperature, as can be noticed from Fig. 6a. These two factors have the common effect of increasing the glycerol mass flow rate, since higher bed temperatures also resulted in higher injection rates to maintain the same residence time with reduced values of syngas density. Two major sources of irreversibilities within the reactor were hypothesised in order to explain the role of the glycerol inflow rate upon reactor efficiency. The first would be the temperature difference between reactants and hot exhaust gases, while the second would be the chemical irreversibility inherent to the reforming reactions.

Higher glycerol concentrations lead to an increase in the temperatures of the vaporisation and inlet zones of the reactor bed and, at the same time, to a reduction in the hot exhaust gases temperatures by demanding a higher amount of energy to sustain the endothermic reforming reactions in comparison to water heating and vaporising. Both effects contribute to a better matching of the temperature of the heat source (combustion product gases) and the reforming temperature, which reduces the amount of exergy destroyed in the reforming/heat transfer processes as pointed out by Simpson and Lutz [58]. Furthermore, the higher amount of energy demanded by the reaction bed will also reduce the exergy loss at the exhaust gases outflow as the glycerol feed ratio increases.

On the other hand, the dilution effect of water vapour reduces the irreversibility rate of the reforming reactions and, thus, the parcel of the irreversibility inherent to the reforming reactions is expected to increase with the glycerol to water feed ratio. An interesting insight on the magnitude of the vaporising, heating and chemical reaction irreversibility effects can be found in the work dedicated to the ethanol reforming by Casas-Ledón et al. [59]. These authors simulated the reforming process by dividing it in individual steps occurring at four separated systems: reactants mixing, vaporising, heating and chemical reforming. Their results indicate that increasing the ethanol feed concentration from 25 to 50% by mass would lead to a minor reduction in the irreversibility parcel associated to the chemical reactions, which represents only 7% of the irreversibility increase experienced by the vaporising and heating parcels. Our experimental results suggest that from 10 to 70% glycerol feed ratio the heating and vaporisation effects also predominated and the reactor efficiency (η_R) was increased with the glycerol feed ratio. However, at 90% glycerol feed concentration the reforming reactions failed to advance and the methanation mechanism predominated, as can be seen in Fig. 4, what reduced the exergy extraction from the hot exhaust gases and

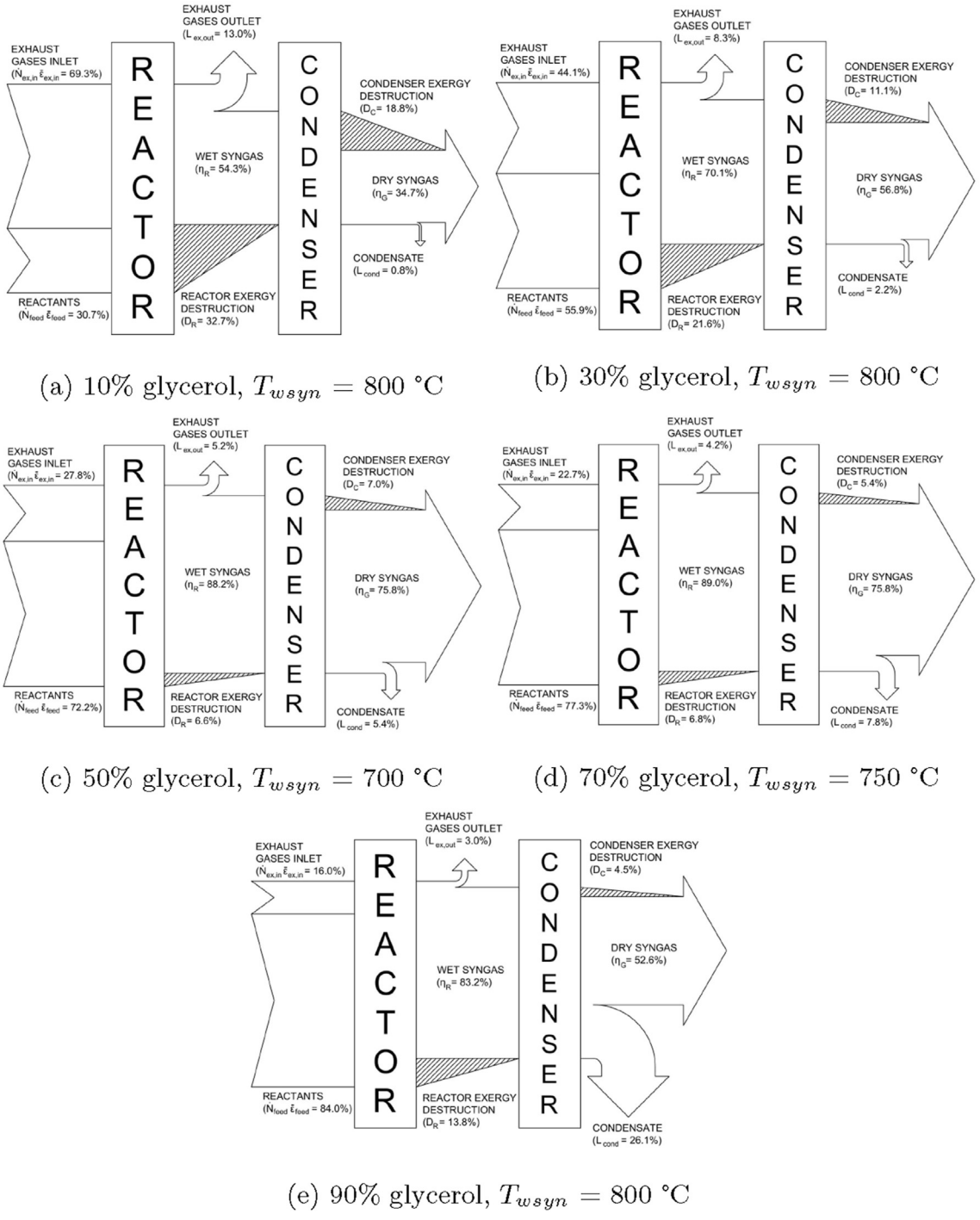

Fig. 8 – Sankey-Grassmann diagrams corresponding to the reactor outlet temperatures T_{wsyn} of maximum exergy efficiency in each feed concentration.

also caused high chemical irreversibilities that penalised the exergy efficiency of the reforming process.

As can be seen from Fig. 6b, the condenser exergy efficiency did not perform well for extreme values of feed ratio. Low efficiency values were registered for 10% glycerol due to the irreversibility associated to the condensation of a high amount of water, while for the 90% glycerol regime the tar losses due to lower reforming reaction progress imposed an appreciable efficiency penalty.

The global reforming efficiency data shown in Fig. 7 reflects the combination of the aforementioned factors, with the regimes corresponding to 50 and 70% glycerol feed ratios achieving the higher global exergy efficiency levels. A plateau of about 75% of global exergy efficiency was observed from 650 °C of reactor outlet temperature, a value that proved sufficient to promote the reforming reactions and restrain methanation effects. These results agree with the maximum

exergy efficiency of 78.23% reported by Dilmac and Ozkan for industrial biogas steam reforming [60].

With regards to glycerol reforming, available literature data indicate a maximum exergy efficiency of 66.1% at 827 °C and 54% of glycerol feed ratio [39]. It is worth to mention that this exergy efficiency was based on equilibrium calculations and defined exclusively based on the hydrogen contribution to the exergy value of the syngas. At this same hydrogen exergy basis, the maximum exergy efficiency obtained in the present study would be reduced to 26,0% being achieved at 70% glycerol feed ratio and 800 °C. In spite of the discordance against equilibrium predictions, our results agreed reasonably well with experimental data reported to ethanol steam reforming that indicate a maximum hydrogen based exergy efficiency of 24.0% [44].

Exergy balances

Further insight regarding the overall system performance can be obtained from exergy balances applied to the reforming reactor and liquid separator. In the interests of simplicity and clarity, the description that follows is limited to the outlet reactor temperatures that maximised η_G for each glycerol feed concentration, whereas the exergy balances are represented by the Sankey-Grassmann diagrams depicted in Fig. 8. As it can be noticed from this figure, the reforming reactor receives two exergy inputs corresponding to the hot gases and feed streams, providing the wet-syngas flow as its useful output. Two thermodynamics imperfections are present within the reforming reactor: The internal irreversibilities and an exergy loss associated to the exhaust gas that is discharged to the surroundings. In the condenser or liquid separator, the exergy input associated to the wet syngas is derived in three terms: A useful dry syngas output, a term of exergy destruction due to the irreversibilities associated to the cool-down of the wet syngas to ambient temperature (D_C), and a term corresponding to the exergy lost due to non-volatile tar condensates and solid char (L_{cond}).

As discussed before, the glycerol content within the reactants improved the heat recovery from the engine exhaust gases and, for that reason, simultaneously reduced the exergy destruction (irreversibilities) within the reforming reactor and the hot exhaust gases exergy losses. Thus, the amount of exergy loss through the exhaust gases outlet ranged from 13 to 3% of the total exergy input, while the exergy destruction ranged from 51.6 to 18.3% as the glycerol feed concentration was increased from 10 to 90% in water. On the other hand, water content within the reaction bed has shown to play an important role in the reforming reaction progress, what imposed an operational limit to the glycerol feed concentration levels. When translated into an exergy balance perspective, the lower levels of reforming reaction completion observed with higher glycerol feed concentrations intensified the exergy losses associated to tar and char formation. From 10 to 70% glycerol in water the condensate tar and char losses increased from 0.7 to 7.8% of the total exergy input, while for 90% glycerol such losses corresponded to 26.1% of the exergy input. A trade-off between the exergy destruction within the system due to irreversibilities and the exergy losses associated to the concentrations of tar and char in the output products was evidenced and, from the obtained data, 50% glycerol in water has proven to be the best operational condition reaching high exergy efficiency values from temperatures above 700 °C.

Still regarding Fig. 8, it is possible to notice that the hot gases exergy input was reduced from 69.3 to 16% of the total exergy input as the feed water content was diminished from 90 to 10% wt, while in the most efficient regimes the hot gases exergy input was responsible for a quarter of the total exergy demanded by the system. From these results it can be speculated that the efficiency benefits of the heat-recovery strategy more than compensate the slight reduction experienced in hydrogen yield due to the non-homogeneous reactor temperature profile. Considering the most efficient operational conditions, it is also interesting to point out that only 5.4–7.0% of the total exergy input was destroyed in the condenser to cool-down the wet syngas and extract the liquid fraction, thus limiting the margin for efficiency gains by recovering some of the exergy destroyed in the condenser to pre-heat the reforming water inlet stream.

From the previous discussion, it is evident that the reforming temperature should guarantee a suitable degree of reaction advance in order to provide an adequate matching between the stream temperatures at the reforming reactor and to avoid excessive tar and char formation, while simultaneously maintaining a tolerable value to limit the irreversibility in the liquid separator. From Fig. 8c and d it can be noticed that the reactor outlet temperatures corresponding to maximum exergy efficiency were 700 and 750 °C at 50 and 70% glycerol feed concentrations, respectively. Conversely, for the remaining of the studied feed concentrations lower levels of exergy efficiency were obtained even at 800 °C. These results suggest that the use of catalysts or other means to boost the reforming reaction advance at lower temperatures would lead to simultaneous reductions in the major imperfections of the studied system: the irreversibilities within the reactor and the condenser and the exergy losses associated to the tar and hot exhaust gases.

Conclusion

The glycerol steam reforming was studied by means of small-scale experiments and its degree of thermodynamic perfection was analysed through the exergy analysis method. The experiments evidenced the preponderant role of the reactants feed concentration with 50%–70% glycerol by weight achieving a coincident maximum exergy efficiency value of 75.8%. As for the syngas exergy content, a maximum value of 24.3 MJ/kg was registered at 50% glycerol feed concentration and 800 °C. This value represents 136.2% of the original glycerol exergy content, constituting an important gain in combustion applications. About a quarter of the total exergy input demanded by the reforming system was recovered from hot exhaust gases, what proved to be an interesting option with regards to energy conservation. At the same time, the bed temperature profile resulting from this option provided a slightly inferior hydrogen yield in comparison to data reported to uniformly heated reactors.

The extent of the considered thermodynamic imperfections, namely the reactor irreversibility, condenser irreversibility, exhaust gases losses and tar/char losses was very similar at maximum efficiency conditions, ranging from 4.2 to 7.8% of the total exergy demanded for the system operation. The importance of reactor improvements in order to reach higher levels of reforming reaction advance/hydrogen yield was confirmed by the exergy analysis, which concluded that such improvements would promote a simultaneous reduction of the main components irreversibilities and of the exergy losses associated to exhaust gases and tar/char formation.

Declaration of competing interest

The authors declare that they have no known competing financial interests or personal relationships that could have appeared to influence the work reported in this paper.

Acknowledgements

This study is supported by the National Council for Scientific and Technological Development of Brazil (No. 574640).

REFERENCES

[1] I. E. Agency. World energy outlook 2019. 2019.
[2] Musa SD, Zhonghua T, Ibrahim AO, Habib M. China's energy status: a critical look at fossils and renewable options. Renew Sustain Energy Rev 2018;81:2281–90.
[3] Agarwal AK. Biofuels (alcohols and biodiesel) applications as fuels for internal combustion engines. Prog Energy Combust Sci 2007;33(3):233–71.
[4] Veljković VB, Biberdžić MO, Banković-Ilić IB, Djalović IG, Tasić MB, Nježić ZB, Stamenković OS. Biodiesel production from corn oil: a review. Renew Sustain Energy Rev 2018;91:531–48.
[5] Sandouqa A, Al-Hamamre Z. Energy analysis of biodiesel production from jojoba seed oil. Renew Energy 2019;130:831–42.
[6] Hajjari M, Tabatabaei M, Aghbashlo M, Ghanavati H. A review on the prospects of sustainable biodiesel production: a global scenario with an emphasis on waste-oil biodiesel utilization. Renew Sustain Energy Rev 2017;72:445–64.
[7] Banković-Ilić IB, Stojković IJ, Stamenković OS, Veljkovic VB, Hung Y-T. Waste animal fats as feedstocks for biodiesel production. Renew Sustain Energy Rev 2014;32:238–54.
[8] Chen J, Li J, Dong W, Zhang X, Tyagi RD, Drogui P, Surampalli RY. The potential of microalgae in biodiesel production. Renew Sustain Energy Rev 2018;90:336–46.
[9] Rathore V, Newalkar BL, Badoni R. Processing of vegetable oil for biofuel production through conventional and non-conventional routes. Energy for Sustainable Development 2016;31:24–49.
[10] Crudo D, Bosco V, Cavaglià G, Grillo G, Mantegna S, Cravotto G. Biodiesel production process intensification using a rotor-stator type generator of hydrodynamic cavitation. Ultrason Sonochem 2016;33:220–5.
[11] Kumar G, Saratale RG, Kadier A, Sivagurunathan P, Zhen G, Kim S-H, Saratale GD. A review on bio-electrochemical systems (bess) for the syngas and value added biochemicals production. Chemosphere 2017;177:84–92.
[12] Ambat I, Srivastava V, Sillanpää M. Recent advancement in biodiesel production methodologies using various feedstock: a review. Renew Sustain Energy Rev 2018;90:356–69.
[13] Escapa A, Manuel MF, Morán A, Gómez X, Guiot SR, Tartakovsky B. Hydrogen production from glycerol in a membraneless microbial electrolysis cell. Energy Fuels 2009;23(9):4612–8.
[14] Schwengber CA, Alves HJ, Schaffner RA, da Silva FA, Sequinel R, Bach VR, Ferracin RJ. Overview of glycerol reforming for hydrogen production. Renew Sustain Energy Rev 2016;58:259–66.
[15] Anuar MR, Abdullah AZ. Challenges in biodiesel industry with regards to feedstock, environmental, social and sustainability issues: a critical review. Renew Sustain Energy Rev 2016;58:208–23.
[16] Cornejo A, Barrio I, Campoy M, Lázaro J, Navarrete B. Oxygenated fuel additives from glycerol valorization. main production pathways and effects on fuel properties and engine performance: a critical review. Renew Sustain Energy Rev 2017;79:1400–13.
[17] Monteiro MR, Kugelmeier CL, Pinheiro RS, Batalha MO, da Silva César A. Glycerol from biodiesel production: Technological paths for sustainability. Renew Sustain Energy Rev 2018;88:109–22.
[18] Saladini F, Patrizi N, Pulselli FM, Marchettini N, Bastianoni S. Guidelines for emergy evaluation of first, second and third generation biofuels. Renew Sustain Energy Rev 2016;66:221–7.
[19] He QS, McNutt J, Yang J. Utilization of the residual glycerol from biodiesel production for renewable energy generation. Renew Sustain Energy Rev 2017;71:63–76.
[20] Chozhavendhan S, Devi GK, Bharathiraja B, Kumar RP, Elavazhagan S. 9 - assessment of crude glycerol utilization for sustainable development of biorefineries. In: Kumar RP, Gnansounou E, Raman JK, Baskar G, editors. Refining biomass residues for sustainable energy and bioproducts. Academic Press; 2020. p. 195–212.
[21] Pompeo F, Santori G, Nichio NN. Hydrogen and/or syngas from steam reforming of glycerol. study of platinum catalysts. Int J Hydrogen Energy 2010;35(17):8912–20.
[22] Bueno AV, de Oliveira MLM. Glycerol steam reforming in a bench scale continuous flow heat recovery reactor. Int J Hydrogen Energy 2013;38(32):13991–4001.
[23] Mehrpooya M, Ghorbani B, Abedi H. Biodiesel production integrated with glycerol steam reforming process, solid oxide fuel cell (sofc) power plant. Energy Convers Manag 2020;206:112467.
[24] Ziyai MR, Mehrpooya M, Aghbashlo M, Omid M, Alsagri AS, Tabatabaei M. Techno-economic comparison of three biodiesel production scenarios enhanced by glycerol supercritical water reforming process. Int J Hydrogen Energy 2019;44(33):17845–62.
[25] Cormos A-M, Cormos C-C. Techno-economic and environmental performances of glycerol reforming for hydrogen and power production with low carbon dioxide emissions. Int J Hydrogen Energy 2017;42(12):7798–810.
[26] Mattson J, Langness C, Niles B, Depcik C. Usage of glycerin-derived, hydrogen-rich syngas augmented by soybean biodiesel to power a biodiesel production facility. Int J Hydrogen Energy 2016;41(38):17132–44.
[27] Silva JM, Soria M, Madeira LM. Challenges and strategies for optimization of glycerol steam reforming process. Renew Sustain Energy Rev 2015;42:1187–213.
[28] Cortright RD, Davda RR, Dumesic JA. Hydrogen from catalytic reforming of biomass-derived hydrocarbons in liquid water. Nature 2002;418(6901):964–7.

[29] Chen H, Ding Y, Cong NT, Dou B, Dupont V, Ghadiri M, Williams PT. A comparative study on hydrogen production from steam-glycerol reforming: thermodynamics and experimental. Renew Energy 2011;36(2):779–88.
[30] Sad M, Duarte H, Vignatti C, Padró C, Apesteguía C. Steam reforming of glycerol: hydrogen production optimization. Int J Hydrogen Energy 2015;40(18):6097–106.
[31] Bobadilla L, Álvarez A, Domínguez M, Romero-Sarria F, Centeno M, Montes M, Odriozola J. Influence of the shape of ni catalysts in the glycerol steam reforming. Appl Catal B Environ 2012;123–124:379–90.
[32] Macedo MS, Soria M, Madeira LM. Glycerol steam reforming for hydrogen production: traditional versus membrane reactor. Int J Hydrogen Energy 2019;44(45):24719–32.
[33] Delparish A, Koc S, Caglayan BS, Avci AK. Oxidative steam reforming of glycerol to synthesis gas in a microchannel reactor. Catal Today 2019;323:200–8.
[34] Chen D, Wang W, Liu C. Hydrogen production through glycerol steam reforming over beehive-biomimetic graphene-encapsulated nickel catalysts. Renew Energy 2020;145:2647–57.
[35] Feng P, Huang K, Xu Q, Qi W, Xin S, Wei T, Liao L, Yan Y. Ni supported on the cao modified attapulgite as catalysts for hydrogen production from glycerol steam reforming. Int J Hydrogen Energy 2020;45(15):8223–33.
[36] S. Moogi, L. Nakka, S. P. Potharaju, A. Ahmed, A. Farooq, S.-C. Jung, G. H. Rhee, Y.-K. Park, Copper promoted co/mgo: a stable and efficient catalyst for glycerol steam reforming, Int J Hydrogen Energy.
[37] Pashchenko D, Gnutikova M, Karpilov I. Comparison study of thermochemical waste-heat recuperation by steam reforming of liquid biofuels. Int J Hydrogen Energy 2020;45(7):4174–81.
[38] Hajjaji N, Baccar I, Pons M-N. Energy and exergy analysis as tools for optimization of hydrogen production by glycerol autothermal reforming. Renew Energy 2014;71:368–80.
[39] Hajjaji N, Chahbani A, Khila Z, Pons M-N. A comprehensive energy–exergy-based assessment and parametric study of a hydrogen production process using steam glycerol reforming. Energy 2014;64:473–83.
[40] Szargut J, Morris D, Steward F. Exergy analysis of thermal, chemical, and metallurgical processes. New York, NY: Hemisphere Publishing; 1988.
[41] Chen Z, Gao L, Han W, Zhang L. Energy and exergy analyses of coal gasification with supercritical water and o2-h2o. Appl Therm Eng 2019;148:57–63.
[42] González WA, Zimmermann F, Pérez JF. Thermodynamic assessment of the fixed-bed downdraft gasification process of fallen leaves pelletized with glycerol as binder. Case Studies in Thermal Engineering 2019;14:100480.
[43] Khila Z, Baccar I, Jemel I, Houas A, Hajjaji N. Energetic, exergetic and environmental life cycle assessment analyses as tools for optimization of hydrogen production by autothermal reforming of bioethanol. Int J Hydrogen Energy 2016;41(39):17723–39.
[44] Hedayati A, Corre] OL, Lacarrière B, Llorca J. Experimental and exergy evaluation of ethanol catalytic steam reforming in a membrane reactor. Catal Today 2016;268:68–78.
[45] Holman JP. Experimental methods for engineers. 8th ed. New York: McGraw-Hill; 2011.
[46] Yildiz G, Lathouwers T, Toraman HE, van Geem KM, Marin GB, Ronsse F, van Duren R, Kersten SRA, Prins W. Catalytic fast pyrolysis of pine wood: effect of successive catalyst regeneration. Energy Fuels 2014;28(7):4560–72.
[47] Dou B, Dupont V, Rickett G, Blakeman N, Williams PT, Chen H, Ding Y, Ghadiri M. Hydrogen production by sorption-enhanced steam reforming of glycerol. Bioresour Technol 2009;100(14):3540–7.
[48] Gallo W, Milanez L. Choice of a reference state for exergetic analysis. Energy 1990;15(2):113–21.
[49] Stein YS, Antal MJ, Jones M. A study of the gas-phase pyrolysis of glycerol. J Anal Appl Pyrol 1983;4(4):283–96.
[50] Valliyappan T, Ferdous D, Bakhshi NN, Dalai AK. Production of hydrogen and syngas via steam gasification of glycerol in a fixed-bed reactor. Top Catal 2008;49(1):59–67.
[51] Aman D, Radwan D, Ebaid M, Mikhail S, van Steen E. Comparing nickel and cobalt perovskites for steam reforming of glycerol. Molecular Catalysis 2018;452:60–7.
[52] Batov DV, Zaichikov AM, Slyusar VP, Korolev VP. Enthalpies of mixing and state of components in aqueous-organic mixtures with nets of hydrogen bonds. Russ J Gen Chem 2001;71(8):1208–14.
[53] Rudakov AM, Sergievskii VV. Activities of the components of glycerol-water binary solutions at 298.15 k. Russ J Phys Chem 2006;80(11):1804–8.
[54] Olikara C, Borman GL. A computer program for calculating properties of equilibrium combustion products with some applications to i.c. engines. In: SAE technical paper. SAE International; 1975.
[55] Bueno AV, Velásquez JA, Milanez LF. Heat release and engine performance effects of soybean oil ethyl ester blending into diesel fuel. Energy 2011;36(6):3907–16.
[56] Kee FMRRJ, Miller JA. Chemkin-ii: a fortran chemical kinetics package for the analysis of gas-phase chemical kinetics. In: Tech. rep. Livermore, CA (USA): Sandia National Labs.; 1989.
[57] D'Avila SG, Silva RSF. Isothermal vapor-liquid equilibrium data by total pressure method. systems acetaldehyde-ethanol, acetaldehyde-water, and ethanol-water. J Chem Eng Data 1970;15(3):421–4.
[58] Simpson AP, Lutz AE. Exergy analysis of hydrogen production via steam methane reforming. Int J Hydrogen Energy 2007;32(18):4811–20.
[59] Casas-Ledón Y, Arteaga-Perez LE, Morales-Perez MC, Peralta-Suárez LM. Thermodynamic analysis of the hydrogen production from ethanol: first and second laws approaches. ISRN Thermodynamics 2012;2012:672691.
[60] Dilmac OF, Ozkan SK. Energy and exergy analyses of a steam reforming process for hydrogen production. Int J Exergy 2008;5(2):241–8.